Mutational Analyses Reveal that the Staphylococcal Immune Evasion Molecule Sbi and Complement Receptor 2 (CR2) Share Overlapping Contact Residues on C3d: Implications for the Controversy Regarding the CR2/C3d Cocrystal Structure

David E. Isenman, Elisa Leung, Julia D. Mackay, Stefan Bagby and Jean M. H. van den Elsen

J Immunol 2010; 184:1946-1955; Prepublished online 18 January 2010;
doi: 10.4049/jimmunol.0902919
http://www.jimmunol.org/content/184/4/1946

The Journal of Immunology is published twice each month by
The American Association of Immunologists, Inc.,
9650 Rockville Pike, Bethesda, MD 20814-3994.

Print ISSN: 0022-1767 Online ISSN: 1550-6606.

Mutational Analyses Reveal that the Staphylococcal Immune Evasion Molecule Sbi and Complement Receptor 2 (CR2) Share Overlapping Contact Residues on C3d: Implications for the Controversy Regarding the CR2/C3d Cocrystal Structure

David E. Isenman,* Elisa Leung,* Julia D. Mackay,† Stefan Bagby,† and Jean M. H. van den Elsen†

We recently characterized an interaction between the *Staphylococcus aureus* immune evasion molecule *Staphylococcus aureus* binder of Ig (Sbi) and complement C3, an interaction mediated primarily through the binding of C3d(g) to Sbi domain IV. Events related to these studies prompted us to investigate via mutagenesis the binding interface of C3d for Sbi domain IV (Sbi-IV), as well as to revisit the controversial issue of the complement receptor 2 (CR2) binding site of C3d. Specifically, we had shown that Sbi domains III and IV fragment binding to C3dg inhibited the latter's binding to CR2. Moreover, a published cocrystal structure of C3d bound to complement inhibitory C-terminal domain of extracellular fibrinogen-binding protein (Efb-C), a structural and functional homolog of Sbi-IV, showed Efb-C binding to a region on the concave face of C3d previously implicated in CR2 binding by our mutagenesis data but not confirmed in the CR2(short consensus repeat [SCR]1–2):C3d cocrystal structure. We have now analyzed by surface plasmon resonance the binding of a series of variant C3dg molecules to biosensor-bound Sbi-IV or CR2(SCR1–2). We found that mutations to the concave face acidic pocket of C3d significantly affected binding to both Sbi-IV and CR2, although there was divergence in which residues were most important in each case. By contrast, no binding defects were seen for mutations made to the sideface of C3d implicated from the cocrystal structure to be involved in binding CR2(SCR1–2). The results with Sbi-IV suggest a mode of binding highly similar to that visualized in the Efb-C:C3d complex. The results with CR2 confirm our earlier mapping studies and cast even further doubt on the physiologic relevance of the complex visualized in the C3d:CR2 cocrystal. ***The Journal of Immunology*****, 2010, 184: 1946–1955.**

In recent years, our understanding of how the human pathogen *Staphylococcus aureus* evades the host innate immune system, and in particular the complement system, has increased through the structural and functional characterization of a number of secreted bacterial virulence factors (1). There are currently six members of this group that collectively target multiple steps in the complement activation pathways. Staphylococcal superantigen-like protein 7 targets C5 and is known to inhibit membrane attack complex-mediated killing (2). Chemotaxis inhibitory protein of *S. aureus* binds to the C5a receptor on host phagocytes, thereby preventing both recruitment and activation of these immune effector cells by complement activation-derived C5a (3, 4). Staphylococcal complement inhibitor binds to both the classical pathway and alternative pathway C3 convertases present on the bacterial surface in a manner that renders them inactive (5, 6). Two homologous proteins, extracellular fibrinogen-binding protein (Efb), and more particularly its C-terminal domain (Efb-C), as well as Efb homologous protein (Ehp), are direct inhibitors of the alternative pathway. Each has been shown to bind to native C3 and induce a conformational change that precludes the latter's participation in alternative pathway propagation (7, 8). Staphylococcal binder of Ig (Sbi) is the most recently characterized of the secreted staphylococcal complement evasion molecules and is also the most complex. The N-terminal–most 266 of its 436 residues are composed of four small globular domains, referred to respectively as Sbi-I, Sbi-II, Sbi-III, and Sbi-IV, and collectively as Sbi-E (9). By contrast, the remainder of the molecule is of unknown domain architecture, although it possesses a proline-rich segment having some sequence similarity to a Gram-positive bacterial cell wall-spanning segment (10). Nevertheless, it lacks the LPXTG segment that is the typical cell wall-anchoring sequence, and in our previous work, we showed that Sbi was absent from the cell wall but was secreted into the surrounding medium (9). Like Efb-C and Ehp, both Sbi-E and its constituent subfragment, Sbi-III-IV, target the human alternative complement pathway. However, the mechanism through which Sbi-E or Sbi-III-IV mediate their anticomplementary activity is very different from that of Efb-C or Ehp, because they induce a futile consumption of C3 in the fluid phase via

*Department of Biochemistry, University of Toronto, Toronto, Ontario, Canada; and †Department of Biology and Biochemistry, University of Bath, Bath, United Kingdom

Received for publication September 4, 2009. Accepted for publication December 3, 2009.

This work was supported in part by Canadian Institutes of Health Research Grant MOP-7081; bridging funds from the Faculty of Medicine, University of Toronto (to D.E.I.); and Biotechnology and Biological Sciences Research Council (U.K.) Follow-on Fund Grant BB/F528014/1 (to J.M.H.v.E. and S.B.).

Address correspondence and reprint requests to Dr. David E. Isenman, Department of Biochemistry, University of Toronto, 1 King's College Circle, Toronto, Ontario M5S 1A8, Canada or Dr. Jean. M.H. van den Elsen, Department of Biology and Biochemistry, University of Bath, Claverton Down, Bath BA2 7AY, United Kingdom. E-mail addresses: d.isenman@utoronto.ca or bssjmhve@bath.ac.uk

The online version of this article contains supplemental material.

Abbreviations used in this paper: b.s.a., buried surface area; CD, circular dichroism; CR2, complement receptor 2; Efb, extracellular fibrinogen-binding protein; Efb-C, complement inhibitory C-terminal domain of Efb; Ehp, Efb homologous protein; NMR, nuclear magnetic resonance; RU, response unit; Sbi, *Staphylococcus aureus* binder of Ig; Sbi-E, Sbi domains I–IV; SCR, short consensus repeat; SPR, surface plasmon resonance; WT, wild-type.

www.jimmunol.org/cgi/doi/10.4049/jimmunol.0902919

alternative pathway activation. This activation is dependent on the presence of the Sbi-III domain, because Sbi-IV does not induce alternative pathway activation but, like Efb-C and Ehp, is an inhibitor of the human alternative pathway, albeit with considerably lower potency on a molar basis (9, 11).

Sbi-IV shares both structural and functional similarities with Efb-C and Ehp. For all three molecules, the primary binding site within C3 is in the C3d/thioester domain (7–9), although in the case of Ehp, there are both high-affinity and low-affinity binding sites for C3d (or C3dg)[1]. X-ray crystallographic (7, 8) and nuclear magnetic resonance (NMR) (11) structure determinations have revealed that Efb-C, Ehp, and Sbi-IV share a common three-helix bundle fold of identical topology. In the case of Efb-C and Ehp, structures of their respective high-affinity complexes with C3d have also been determined and in both cases show that several basic residues of helix 2, as well as an asparagine residue of this helix, are in close contact with an acidic-residue–lined pocket on the concave surface of the dome-shaped C3d molecule (7, 8). Indeed, the R131A/N138A combination mutant of Efb-C, which encompasses two of the prominent C3d-contacting residues in helix 2, abolished the interaction of Efb-C with C3d (7). Mutating the equivalent residues of Ehp abolished the high-affinity interaction with C3d (8). Although the sequence identity between Efb-C and Sbi-IV is low (~19%), R231and N238 of Sbi-IV align with R131 and N138 of Efb-C, and we found that mutating either of these Sbi-IV helix 2 residues to alanine resulted in total loss of C3dg-binding activity (11).

The C3d (or C3dg) fragment on its own, or as part of the precursor C3 degradation fragment iC3b, is the ligand for complement receptor 2 ([CR2]/CD21) present on B cells and follicular dendritic cells (14). CR2 on these cells exists as a complex with CD19 (15), a well-characterized signaling platform, and with CD81 (16), a tetraspanning membrane protein that through inducible palmitoylation can target the CR2/CD19/CD81 complex to lipid rafts (17, 18). The coligation of the BCR complex with the CR2/CD19/CD81 complex by Ag opsonized with C3d(g) colocalizes both receptors to lipid rafts, and this in turn both augments and prolongs B cell signaling (19). This phenomenon, as well as the ability of CR2 present on follicular dendritic cells to trap C3dg-opsonized Ag and present it to somatically hypermutating B centrocytes in the germinal center (20), in large part explains the molecular adjuvant role for complement in obtaining an optimal Ab response to T-dependent Ag (21, 22). We have previously shown that the binding of Sbi-III-IV to C3dg was inhibitory to the latter's interaction with the C3d-binding domains of CR2, namely short consensus repeat domains 1 and 2 (CR2 [short consensus repeat (SCR)1–2]), and that this inhibition appeared to be competitive (9). Because Sbi-III shows no binding activity toward any C3 derivative (9) and because the binding constants of Sbi-III-IV and Sbi-IV for C3dg are essentially identical (9, 11), the inhibition of CR2 binding may logically be assumed to be due to the interaction of Sbi-IV with C3dg. Recently, the CR2:C3d interaction was also shown to be inhibited by the binding of Efb-C to C3d (23). On the one hand, these observations collectively indicate that Sbi, Efb, and Ehp interfere with complement's role in both the innate and adaptive branches of the host immune system. However, given our knowledge of where Efb-C binds C3d (7), these observations also connect the issue of the Sbi-IV contact site on C3d to a controversy in the literature regarding the CR2 binding site of C3d (24–26). Specifically, a cocrystal structure of a complex between C3d and CR2(SCR1–2) (26) indicates a contact interface on the C3d molecule that is completely discordant with one involving the acidic residue-lined depression on the concave surface of C3d that had been deduced from earlier site-directed mutagenesis studies (24). However, the latter interface is precisely the one visualized as the area of contact between C3d and the predominantly basic residues of the middle helices of both Efb-C (7) and Ehp (8).

Given both the structural and functional similarities of Sbi-IV to Efb-C and Ehp, we wished to obtain mutagenic validation that the same interface of C3d is also used in binding Sbi-IV as has been visualized in the cases of the complexes with Efb-C and Ehp. In this study, we have obtained such data by generating a series of mutants of recombinant C3dg and measured their relative binding activities to Sbi-IV by surface plasmon resonance (SPR). Given the connection of this issue to that of the controversy regarding the location of the CR2 binding site in C3d, we have also examined by SPR the same series of mutant C3dg molecules for their ability to bind to CR2(SCR1–2). Our findings strongly suggest that Sbi-IV binds to the same region of C3d as do Efb-C and Ehp. The results with CR2 binding confirm by independent means our earlier mapping study and cast even further doubt on the physiologic relevance of the complex visualized in the C3d:CR2 cocrystal.

Materials and Methods

Proteins

The expression and purification of Sbi-IV has been described previously (9). The soluble human CR2(SCR1–2) used in this study is the mammalian cell culture-derived $(CR2)_2$-$IgG1_{mouse}$ fusion protein described by Hebbel et al. (27). As such, the CR2(SCR1–2) entity would possess its normal mammalian carbohydrate chains at Asn residues 101 and 107 of SCR2. It has previously been noted (28) that the unusual V-shaped folded-back arrangement of SCR1 and SCR2 seen in the X-ray crystal structures of both free CR2(SCR1–2) (28), and in its complex with C3d (26), would not be possible due to severe steric clashes between carbohydrate and SCR1 had a typical length mammalian glycan chain been attached to Asn^{107}. By choosing to use the mammalian cell-derived CR2(SCR1–2) construct, as opposed to a bacterially expressed construct of the same domains, we avoid the potential complication to the interpretation of our binding experiments of the unphysiologic conformation having the possibility of being adopted. Culture conditions for the J558L-pSNRCR2 line secreting $(CR2)_2$-IgG1 were as described previously (24), and the harvested culture supernatants were dialyzed against 10 mM sodium phosphate and 0.15 M NaCl (pH 7.2) (loading/wash buffer). $(CR2)_2$-IgG1 was absorbed from 100 ml of the dialyzed culture medium, containing ~100 μg of the soluble CR2 fusion protein, onto an Affigel-10 column bearing 3 mg of covalently coupled recombinant C3d, where the latter was expressed and purified as described previously (12). Following extensive washing of the column, $(CR2)_2$-IgG1 was eluted using the same buffer adjusted to 1 M NaCl. Purity was assessed by SDS-PAGE under reducing conditions.

Construction of the mutant forms of human C3dg fell into two categories: those for which the mutants already existed in the context of the intact C3 cDNA mammalian expression vector pSV-C3(LC) (24), and those which were made de novo for this study. pET-15bC3dg(oligoHis$^-$) represents a modified bacterial pET15b expression in which the N-terminal His6-tag and the thrombin cleavage site encoded by the vector had been deleted and in which, in addition to the vector-encoded sequence MLE, the C3 residues encoded are D948 (prepro numbering) through R1323. For the existing mutants, which represented mostly alanine mutations targeting residues on the concave surface of C3d (24), this cDNA segment was PCR amplified using the appropriate pSV-C3(LC) template DNA, a forward primer positioned to take advantage of an endogenous BamHI site at nucleotide 2901 (this yields an in-frame product extending seven codons upstream of the the codon for E955 marking the fI-delimited N terminus of C3dg) and

[1]As a point of clarification regarding fragment nomenclature, C3dg is a 348-residue physiologic degradation fragment of C3b that results from three successive proteolytic cleavages by the regulatory enzyme fI in the presence of CR1 as a fI cofactor. C3d is a proteolytic limit fragment of C3 digestion and, depending on the protease used, is lacking 33–47 residues from the N terminus of C3dg. The boundaries of the commonly used recombinant C3d fragment (12) correspond fairly closely to the thioester domain visualized in the structure of C3b (13). The additional 46-residue N-terminal extension of recombinant C3d that is present in recombinant C3dg is derived from the g segment of the CUB domain that is visualized in the C3b structure. However, in the absence of the remainder of the CUB domain, this polypeptide extension is likely to be unfolded. In terms of binding to CR2, recombinant C3d and recombinant C3dg have been shown to be equivalent (12).

a reverse primer that encodes two stop codons immediately after the codon for R1323 (the fI-delimited C terminus of C3dg), plus a sequence encoding a BamHI restriction site. Vent polymerase (New England Biolabs, Beverly, MA) was used for all PCR amplifications. The BamHI-restricted PCR product was then cloned into the unique BamHI site in the polylinker of pET15b (oligoHis$^-$), and transformant plasmids having the desired orientation were ascertained by diagnostic restriction analysis. The new alanine mutants made for this study target residues E1110, D1115, D1121, D1140, and N1163 and were constructed using the overlap–extension PCR method of site-directed mutagenesis (29) using as template wild-type (WT) pET-15bC3dg (oligoHis$^-$). For the first four of the above mutants, a 589-bp EcoRI–SfiI fragment of the mutant PCR product was exchanged for the equivalent fragment in the WT pET-15bC3dg(oligoHis$^-$). For the N1163 mutant, a 223-bp SfiI–AgeI fragment was similarly exchanged. The DNA sequence over the entire coding region of the respective C3dg bacterial expression plasmids was verified for all constructs (DNA Sequencing Service, Center for Applied Genomics, Hospital for Sick Children, Toronto, Ontario, Canada).

The various recombinant C3dg proteins were expressed in the *Escherichia coli* host cell BL21(DE3). One-liter cultures in LB-amp were grown at 37°C to A_{600} of ~0.6, at which time recombinant protein expression was induced with 0.5 mM isopropyl β-D-thiogalactoside at 23°C for ~18 h. Harvested cells in 10 mM sodium phosphate, 0.075 M NaCl, 2 mM EDTA, and 2 mM PMSF (pH 7.2) were disrupted using a French Press. The centrifuged lysate, which contained the vast majority of the recombinant C3dg protein, was dialyzed against 20 mM sodium acetate, 20 mM NaCl, and 1 mM EDTA (pH 5.5) and loaded onto a 100-ml column of CM-Sepharose Fast Flow (GE Health-Pharmacia, Piscataway, NJ). Following extensive washing in loading buffer, conditions under which most of the bacterial proteins eluted, the recombinant C3dg protein was generally eluted in the loading buffer made 0.3 M in NaCl and 0.1 mM DTT. The one exception to this elution condition was for the D1029A/E1030A/E1032A triple mutant where, owing to the large change in intrinsic charge, 2 M NaCl was used to release the C3dg protein. The eluted proteins were dialyzed into 10 mM sodium phosphate, 0.15 M NaCl, and 0.1 mM DTT (pH 7.2), made 4 mM in DTT, concentrated by ultrafiltration to between 10 and 20 mg/ml and stored at −75°C. The recombinant C3dg proteins were ~80% pure at this stage, and the DTT was present to prevent formation of thioester cysteine-mediated covalent dimers. As close as possible to using the series of recombinant C3dg proteins in SPR experiments, 0.5 ml of 4 mg/ml protein was further purified on a Superdex 200 HR 10/30 FPLC size-exclusion column equilibrated in 10 mM HEPES, 0.15 M NaCl, and 3 mM EDTA (pH 7.2) (HBS-E). We estimate from SDS-PAGE analysis conducted under both reducing and nonreducing conditions of the monomer peak that the recombinant C3dg proteins used in the SPR experiments were all ~95% pure and showed no evidence of any covalent dimer being present (Supplemental Fig. 1).

SPR measurements

SPR experiments were performed at 25°C on either a Biacore 3000 or a Biacore-X instrument (Biacore Life Sciences, Piscataway, NJ) in HBS-E containing 0.005% P20 surfactant at a flow rate of 20 μl/min. P-20 surfactant (0.005%) was added to all the gel-filtered C3dg samples prior to their use. Ligands (Sbi-IV or $(CR2)_2$-IgG) were coupled to a CM-5 biosensor chip using standard amino group-coupling chemistry, with flow cell 1 being sham-activated and sham-deactived and acting as a reference channel whose signal is subtracted from the experimental channel(s). Typically, Sbi-IV couplings resulted in immobilized protein levels of ~1100 response units (RU), whereas $(CR2)_2$-IgG immobilization levels ranged in different experiments from 500 to 4800 RU. In the mutant scan experiments, the concentrations of all recombinant C3dg proteins were adjusted to 0.1 mg/ml (2.5 μM), based on an extinction coefficient ($E^{1\%}_{280nm,\ 1cm}$) of 12.6 and a molecular mass of 40.1 kDa. Analyte injections were for 60 s, followed by a 60-s buffer flow at the same rate before the injection loop, and flow cells were washed. The biosensor chip was regenerated between experiments with a 60 s pulse of 2 M NaCl, which brought the sensorgram signal back to baseline. The affinity of WT C3dg for biosensor-bound $(CR2)_2$-IgG was determined by fitting the steady-state plateau RU values of a series of C3dg analyte injections to a single-site Langmuir-binding isotherm by nonlinear regression analysis, as described previously (9). The effect of Sbi-IV coanalyte on this binding curve was assessed as described previously using Sbi-III-IV as the coanalyte (9).

ELISA-based $(CR2)_2$-IgG:C3dg–binding assay

Microtiter wells (Immulon 2; Dynatech Laboratories, Chantilly VA) were coated overnight at 4°C with 100 μl of 15 μg/ml C3dg C1010A in 10 mM sodium carbonate buffer (pH 9.8) or with the carbonate buffer alone for control wells. Blocking was with 5% skim milk in HEPES saline (pH 7.2) containing 0.05% Tween 20, followed by a wash in HEPES saline (pH 7.2). C3dg-coated wells, and corresponding control wells, were incubated for 2 h at room temperature with a 2-fold dilution series of $(CR2)_2$-IgG in either a zinc-containing (0.1 M sodium cacodylate, 0.2 M zinc acetate, and 0.05% Tween 20 [pH 6.26]) or control buffer (0.1 M sodium cacodylate, 0.06 M NaCl, and 0.05% Tween 20 [pH 6.26]). Both of these buffers had a conductivity of 10.5 mS. The first wash following the exposure of the wells to $(CR2)_2$-IgG was done with the respective zinc, or no-zinc buffer, followed by three additional washes in an isoionic no-zinc PIPES saline buffer (15 mM PIPES, 0.105 M NaCl [pH 6.8], and 0.05% Tween 20). Binding of $(CR2)_2$-IgG to experimental and control wells was detected using alkaline-phosphatase–conjugated rabbit anti-mouse IgG (Jackson ImmunoResearch Laboratories, West Grove, PA) by standard methods. The absorbance at 405 nm of each no-coat control well was subtracted from the reading of the corresponding experimental well. The CR2(SCR1–2) dependency of the assay was controlled for by incubating C3dg-coated wells with a mouse IgG1 anti-human HLA-DR (AB2.06; a gift from Dr. T. Watts, Department of Immunology, University of Toronto, Toronto, Ontario, Canada) in a no-zinc buffer at a concentration at the upper end of those used for$(CR2)_2$-IgG. In one confirmatory experiment, an HRP-conjugated goat anti-mouse IgG (Jackson ImmunoResearch Laboratories) was used as an alternative detection Ab, using *ortho*-phenylenediame as the substrate.

CD measurements

Far UV CD spectra were obtained using a Jasco J-810 spectropolarimeter in HBS-E buffer at 20°C. Mean residue ellipticity was calculated using a mean residue weight of 112 for the various recombinant C3dg fragments assessed. In no case did the mutant C3dg spectra deviate significantly from the WT spectrum. Pertinent examples of CD spectra representing variant C3dg molecules from all three regions of the molecule explored through site-directed mutagenesis are shown in Supplemental Fig. 2.

Protein interface calculations

Buried surface areas of protein interfaces derived from published X-ray crystal structures were calculated using the protein interfaces, surfaces, and assembly (PISA) web server (www.ebi.ac.uk/msd-srv/prot_int/pistart.html) at the European Bioinformatics Institute (30).

Results

Sbi-IV inhibits binding of C3dg to CR2(SCR1–2)

We had previously shown that Sbi-III-IV could inhibit the binding of C3dg to CR2(SCR1–2). Because Sbi-III on its own had no C3dg-binding activity, by inference the inhibition was due to the Sbi-IV:C3dg interaction. The experiment shown in Fig. 1*A* directly confirms that this is indeed the case because the presence of Sbi-IV as a co-analyte with C3dg causes a significant inhibition in the binding of C3dg to biosensor-bound CR2(SCR1–2). This inhibition persists so long as Sbi-IV is present in molar excess of C3dg, but at excess C3dg over Sbi-IV, the binding level to CR2(SCR1–2) approaches that seen in the absence of the Sbi-IV coanalyte, as would be expected for a competitive binding situation (Fig. 1*B*). An additional point regarding Fig. 1*A* is that at physiological ionic strength, the binding of C3dg to the mammalian cell-derived $(CR2)_2$-IgG fusion protein that is coupled to the biosensor chip yields a straightforward single-class Langmuir-binding isotherm governed by a K_D of 9.4 μM. Previous reports in the literature had stated that the authors had been unable to obtain a direct binding constant for the CR2-C3d(g) interaction at physiological ionic strength, be it with full-length CR2 (31) or with CR2(SCR1–2) (32). An estimated K_D of 27.5 μM had been reported for full-length soluble CR2 binding to C3d based on extrapolation of ultracentrifugation data obtained at lower ionic strength (31).

Mutation of residues located on the concave face of C3d affect its binding to Sbi-IV and CR2(SCR1–2)

Having established that the binding sites of Sbi-IV and CR2(SCR1–2) on C3d are at the very least sufficiently overlapping to sterically inhibit one another, we wished to determine the extent to which they used the same residue side chains of C3d as major interaction partners. A series of mutant human C3 molecules had previously been created (24), which targeted the acidic residue-lined concave

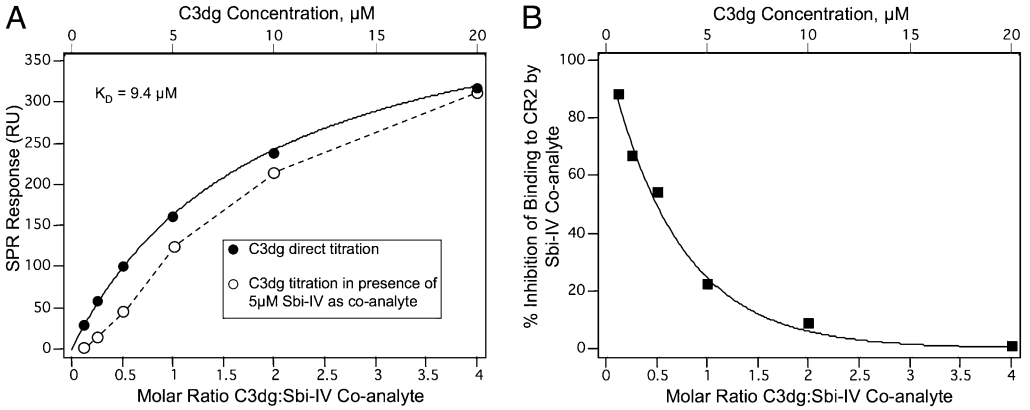

FIGURE 1. Inhibition of binding of C3dg to CR2 by Sbi-IV. *A*, ●, A saturation curve of WT C3dg steady-state plateau level binding to sensor chip-immobilized $(CR2)_2$-IgG fusion protein at physiologic ionic strength. The *upper abscissa* denotes the C3dg concentration and the solid line through ● in *A* represents the fit of the data to a single class of binding site Langmuir-binding isotherm, yielding a K_D of 9.4 μM. ○, The same titration carried out in the presence of 5 μM Sbi-IV as coanalyte. A small nonspecific signal as a result of some interaction of 5 μM Sbi-IV with the $(CR2)_2$-IgG on the chip has been subtracted from each data point of the coanalyte titration. The *bottom abscissa* indicates the molar ratio of C3dg/Sbi-IV at each point of the titration. *B* is an alternative depiction of the inhibition of C3dg binding to CR2 by Sbi-IV. Each ○ data point of *A* is depicted in *B* as percent inhibition of C3dg binding to CR2 relative to the same titration point in the absence of Sbi-IV coanalyte [i.e., percent inhibition = (1 − [RU in presence of Sbi-IV/RU in absence of Sbi-IV]) × 100].

surface of C3d that we had predicted, based on the C3d structure and the known ionic strength dependence of the CR2:C3d interaction (31, 33), was a likely candidate to form at least part of the binding interface with CR2(SCR1–2). In that study, published in 2000, the bulk of the data came from quantitative rosette assays between recombinant iC3b-coated red cells and full-length CR2 on Raji B cells, as well as flow cytometry experiments detecting the binding of the same $(CR2[SCR1–2])_2$-IgG fusion protein used in the current study to the various recombinant iC3b molecules deposited on red cells. Collectively, the experiments identified two clusters of predominantly acidic residues on the concave surface of C3d that appeared to mediate the binding interaction with CR2 (SCR1–2). When the structure of the Efb-C:C3d cocrystal was published (7), it was clear that helix 2 of Efb-C made contacts with several of the residues that existed in our mutant collection. We therefore decided to subclone cDNA segments corresponding roughly to the fI-delimeted C3dg fragments for 12 mutants, to express the recombinant C3dg fragments in bacteria, and to use the biophysical technique of SPR to determine their relative to WT-binding ability to biosensor chip-bound Sbi-IV. Given the controversy regarding the CR2 binding site on C3d, the same series of recombinant C3dg molecules were also assessed by SPR for their relative binding to a biosensor channel coated with the $(CR2[SCR1–2])_2$-IgG fusion protein.

For simplicity of data presentation, the right hand and left hand clusters of the target group of residues on the concave face of C3d are treated separately in Fig. 2*A* and 2*B*, respectively. The location of each target residue is also depicted on a surface rendering of the concave face of C3d (Fig. 2*A*, 2*B*, *rightmost panels*). For ease of reference to the earlier publications on the CR2 (24, 26) and the Efb-C or Ehp (7, 8) binding interfaces, residue numbering on data figures is provided in both the C3d and preproC3 numbering systems, although the text will predominantly use the C3d numbering system. In all cases, relative binding of the variant C3dg molecules to Sbi-IV and to CR2 was assessed at a fixed concentration of 2.5 μM and at physiologic ionic strength. Fig. 2 presents a representative experiment for the complete set of mutants carried out with a single pair of biosensor chips, whereas Fig. 3*A* presents collective means and SDs of relative to WT-binding activity data carried out on several independent biosensor chips of Sbi-IV and CR2(SCR1–2). Finally, Fig. 3*B* presents surface renderings of the C3d structure on which are mapped in a color-coded fashion the effect of a particular mutation on the ability of C3dg to bind to Sbi-IV (*left panel*) and CR2(SCR1–2) (*right panel*).

The effect on Sbi-IV binding of mutations within C3d 30s–40s cluster is shown in the *left panel* of Fig. 2*A*. It can be seen that single loss of charge mutations at the neighboring pair of residues D36 and R49 led to the complete (D36A) or near complete (R49M) loss of Sbi-IV–binding activity (Figs. 2*A*, *left panel*, 3). The E37A mutant shows a less severe but still significant defect in binding of slightly >50%. By contrast, E39 and E42 appear to be outside of the contact region because their mutation to alanine shows a <20% defect, and the defect for the K291A mutant is also quite moderate (~30%), suggesting that it too may be peripheral to the Sbi-IV contact region. The effect of this series of mutations on the ability of the respective C3dg fragments to bind to biosensor-immobilized CR2(SCR1–2) is shown in the *center panel* of Fig. 2*A* and in cumulative data form in Fig. 3. Unlike the case for Sbi-IV binding, there is no single residue within this cluster whose mutation essentially eliminates binding to CR2; however, this was the case for the triple-mutant D36A/E37A/E39A. Of these three residues, the largest defect is due to the loss of the side chain of E39, followed by E37, whereas alanine substitution of E36 leads to a modest 30–40% drop in binding activity. The side chains of neither E42 nor K291 appear to contribute much to the contact with CR2, and although in the experiment shown in Fig. 2*A* the R49M mutation resulted in a 60% defect in CR2 binding, the mean of four experiments suggested a more modest defect of 40%. Clearly, the side chains of residues within the 30s–40s cluster of C3d contribute to both the binding to Sbi-IV and CR2, but whereas residues D36 and R49 in the upper region of the cluster are the most vital for Sbi-IV binding, residues E39 and E37 at the lower end of the cluster contribute the most to CR2 binding (Fig. 3*B*).

As can be seen in both Fig. 2*B*, *left panel*, and in the cumulative data of Fig. 3, alanine mutations of single residues in the 160s cluster give rise to moderate defects on Sbi-IV binding, with only C3dg mutants I164A and D163A having a >2-fold effect on binding. Nevertheless, with the possible exception of E167, which may be outside the contact area for Sbi-IV, the data suggest that residues within the 160s cluster make some contribution to the Sbi-IV–binding interface, although clearly not of an anchoring residue type such as was seen for residues D36 and R42. By contrast, with respect to CR2 binding, four of the five single residue mutations made in the 160s cluster give rise to major

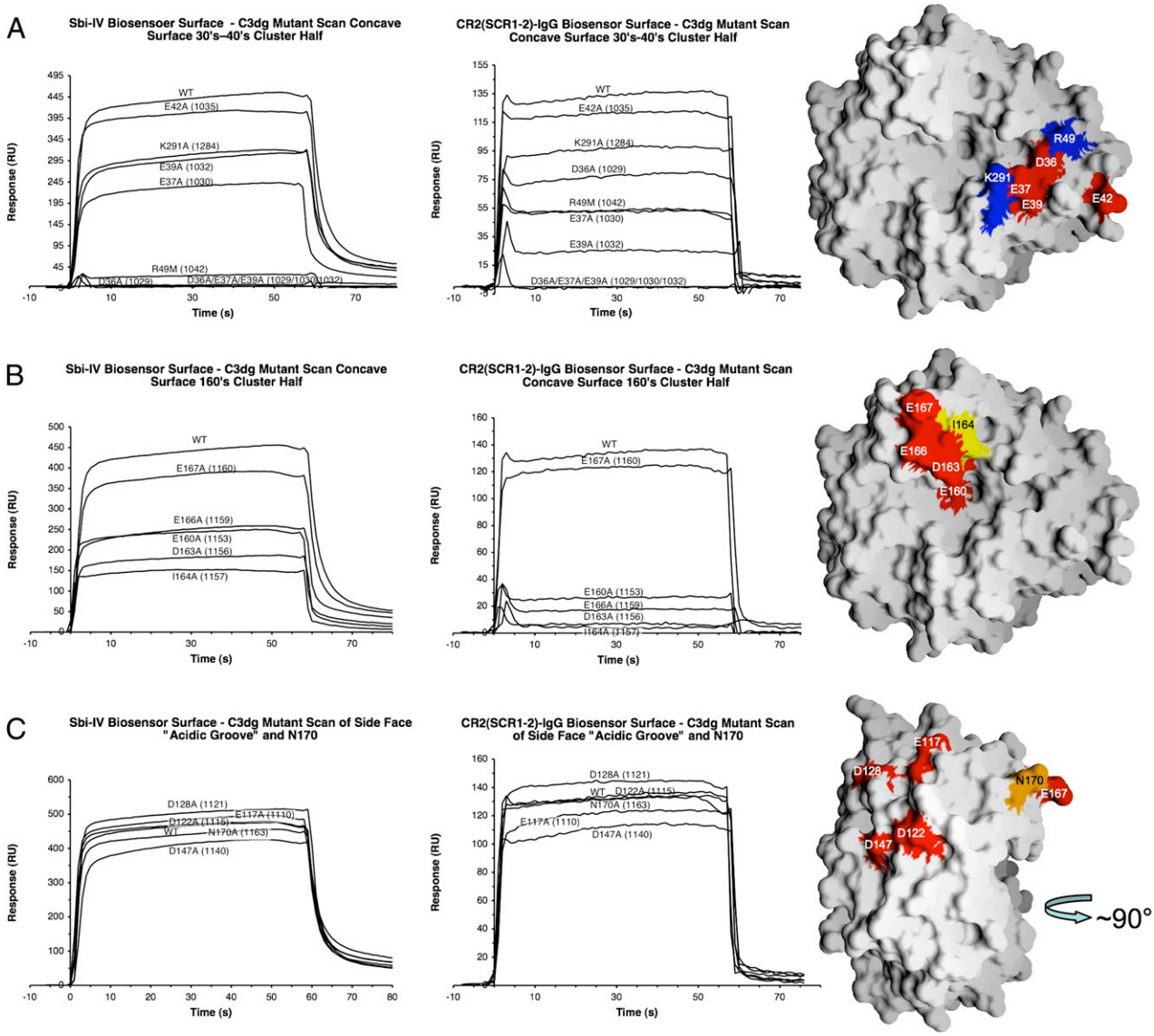

FIGURE 2. Assessment by SPR assay of the relative to WT-binding activities to Sbi-IV (*leftmost panels*) and CR2(SCR1–2) (*center panels*) of mutant C3dg molecules. All injections were at a C3dg concentration of 2.5 μM and under physiologic buffer conditions. *A* shows data for mutations mapping to the 30s–40s cluster of residues on the concave surface of C3d, *B* shows the data for the 160s cluster of residues on the same face of the molecule, and *C* shows data for residues located on a side face of the C3d molecule encompassing the "acidic grove" residues and N170. The *rightmost panels* in each case show the location of the mutants on a surface rendering of the C3d molecule color-coded according to the chemical nature of the side chain (blue, basic; red, acidic; orange, polar noncharged; yellow, hydrophobic). These representative experiments for the complete set of recombinant C3dg molecules analyzed, and for which we show the primary data, were done on a Biacore-X using CM-5 chips that were respectively coupled with 1100 RU of Sbi-IV and 4800 RU of $(CR2)_2$-IgG. The WT sensorgrams for each chip are reproduced in each of *A*, *B*, and *C*. Individual sensorgrams of mutant C3dg are labeled using both preproC3 and C3d numbering, but for clarity, the surface structure figures use only C3d numbering.

binding defects of >80% (Figs. 2*B*, *center panel*, 3). On the basis of the extent of defect seen, D163 (5% of WT activity) and I164 (8% of WT activity) appear to be the most important contact residues, followed by D166 and E160 (17% of WT activity, each). Mutation of residue E167 has a very minimal effect on CR2 binding, suggesting that it is peripheral to the binding interface. Whereas the anchoring contacts for Sbi-IV binding to C3d(g) appear to be in the 30s–40s cluster, those for CR2 appear to reside within the 160s cluster.

Mutation of C3d residues constituting a side face acidic groove and N170 affect neither the binding to CR2 nor Sbi-IV

Two of the most unexpected features of the CR2(SCR1–2):C3d cocrystal structure (26) were first, that only SCR2 was involved in the binding interface to C3d, and second, that the only side chain-side chain interaction visualized was between C3d N170 and CR2 Y80. Main chain carbonyl oxygens mediated the remaining interactions visualized on the C3d side of the interface. These observations contradicted extensive biochemical data implicating both SCR1 and SCR2 in the contact (34, 35). Furthermore, on the basis of the well-established ionic strength dependence of the interaction (31–33), one might have expected to see classical salt bridges in the structure of the complex. Subsequently, the same group that published the CR2(SCR1–2):C3d cocrystal structure showed through mutagenic analysis that a cluster of basic residues on one face of the SCR1 domain was quite important for the binding interaction (36). Although acknowledging that the cocrystal structure represented an incomplete view of the true complex, the group went on to propose that a cluster of residues (E117, D122, D128, and D147) forming an acidic groove on the

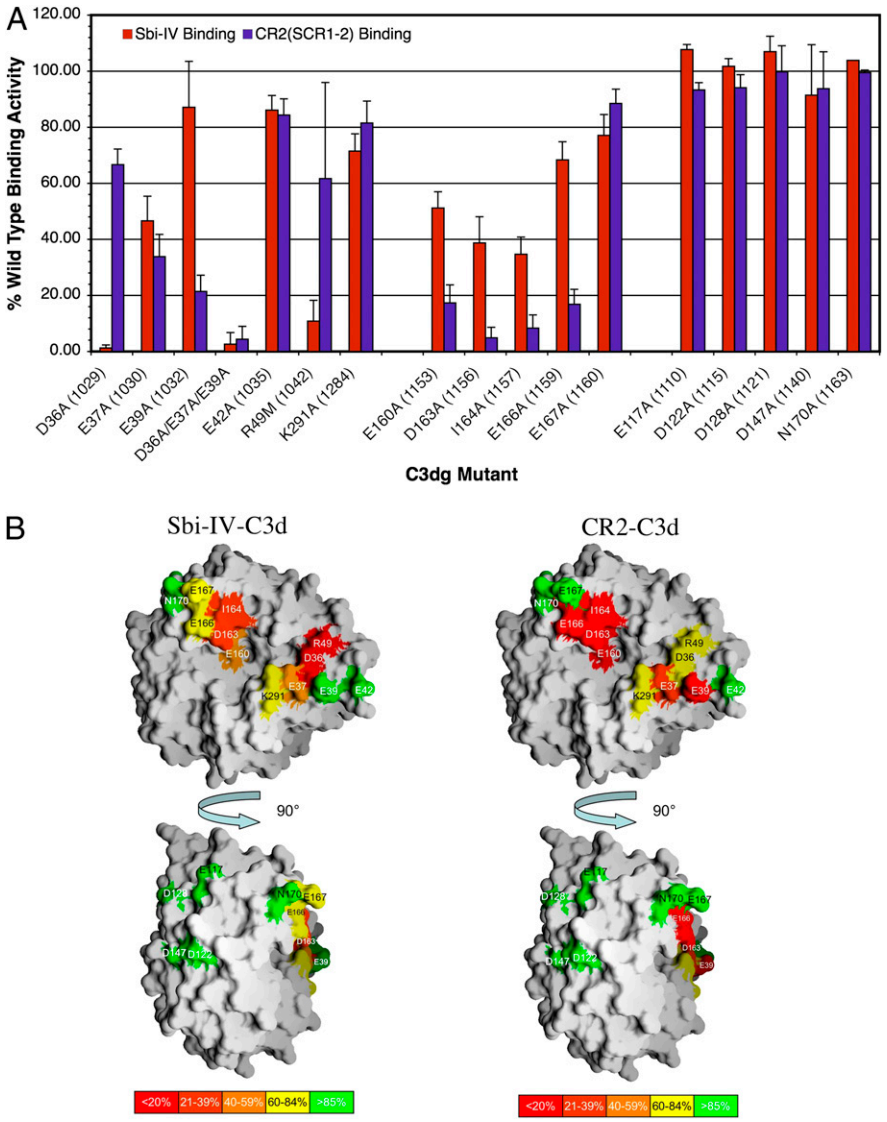

FIGURE 3. Relative to WT-binding activities of mutant C3dg molecules to Sbi-IV and CR2(SCR1–2) derived from replicate SPR experiments, all carried out using 2.5 μM C3dg under physiologic buffer conditions. *A* depicts, in bar graph form, the respective means and SD error bars of percent WT-binding activity to Sbi-IV (red bars) and CR2(SCR1–2) (blue bars). In some cases, the data were from experiments missing a few mutants, which only became available in the later phases of the study. The number of replicate experiments (n) on the Sbi-IV chips is: for D36A, D37A, D39A, D36A/D37A/D39A, E42A, R49M, K291A, E160A, D163A, I164A, E166A, and E167A, $n = 5$; for E117A, D122A, D128A, and D147A, $n = 4$; and for N170A, $n = 1$. The number of replicate experiments on $(CR2)_2$-IgG chips is: for D36A, E37A, D36A/E37A/E39A, E42A, R49M, K291A, E160A, D163A, I164A, and E166A, $n = 4$; for E39A, E167A, E117A, D122A, and D128A, $n = 3$; and for D147A and N170A, $n = 2$. *B* maps the data in *A* onto surface renditions of C3d according to color-coded ranges (see bottom of figure) of relative to WT C3dg-binding activities. *Left panels* depict the binding defect map for the interactions with Sbi-IV and *right panels* for those with CR2(SCR1–2).

same face of C3d as shown to interact with SCR2 in the cocrystal structure was a good candidate to provide the complementary interface for the basic residues of the SCR1 domain. We have now mutated these acidic groove residues to test their hypothesis. It can be seen in Fig. 2*C*, *center panel*, of the representative experiment, and in the cumulative data depicted in Fig. 3, that essentially WT-binding behavior to CR2(SCR1–2) was seen for all four alanine mutants of the residues constituting the acidic groove of C3d. These mutations also had no significant effect on the binding of C3dg to Sbi-IV (Figs. 2*C*, *left panel*, 3). Finally, in our hands, mutating N170 to alanine, thus theoretically removing the ability of this side chain to form an interaction with Y80 of SCR2, had no effect on the binding of C3dg to CR2(SCR1–2). For the sake of completeness, the N170A mutant C3dg was also assessed for its ability to bind to Sbi-IV, but here too the binding activity was identical to WT C3dg (Figs. 2*C*, 3).

Zinc ions inhibit the binding of CR2(SCR1–2) to C3dg

The crystallization conditions reported by Szakonyi et al. (26) for the CR2(SCR1–2):C3d complex were as follows: 17% polyethylene glycol 2000, 0.2 M zinc acetate, and 0.1 M sodium cacodylate (pH 7.36). In fact it is impossible to obtain such a solution at the stated pH as the zinc hydroxide formed is not soluble beyond ~0.5 mM (37). As an additive to a 0.1 M sodium cacodylate buffer titrated to pH 7.36, 0.2 M zinc acetate is soluble, but the pH drops to 6.26. This pH is still above the point where the CR2 (SCR1–2):C3d–binding affinity begins to significantly decrease (32). The measurement of the effect of zinc ion on the C3dg:CR2 (SCR1–2) interaction was assessed using an ELISA-based assay in which, with the exception of the polyethylene glycol precipitant, the binding conditions mimicked those of the crystallization. Variable concentrations of the $(CR2)_2$-IgG fusion protein were offered to wells coated with C3dg, or control noncoated wells, in either a zinc acetate/cacodylate buffer at pH 6.26, or in the same buffer without zinc acetate and made isoionic with NaCl. It can be seen in Fig. 4 that the robust binding interaction observed between $(CR2)_2$-IgG and C3dg in the buffer without zinc acetate is essentially abrogated in the presence of 0.2 M zinc acetate. An irrelevant mouse IgG1 mAb showed no evidence of binding to the C3dg-coated wells (Fig. 4), demonstrating that the binding observed in the absence of zinc acetate was CR2 dependent. Finally, as the ELISA detection enzyme calf intestinal alkaline-phosphatase is known to be significantly inhibited by the presence of micromolar concentrations of zinc ion (38), to preclude the remote possibility that there was sufficient zinc acetate carrying through the washes to be directly inhibiting the detecting enzyme, the assay was repeated using an HRP-conjugated goat anti-mouse IgG detection Ab. Zinc ions, if present after the washes, would actually

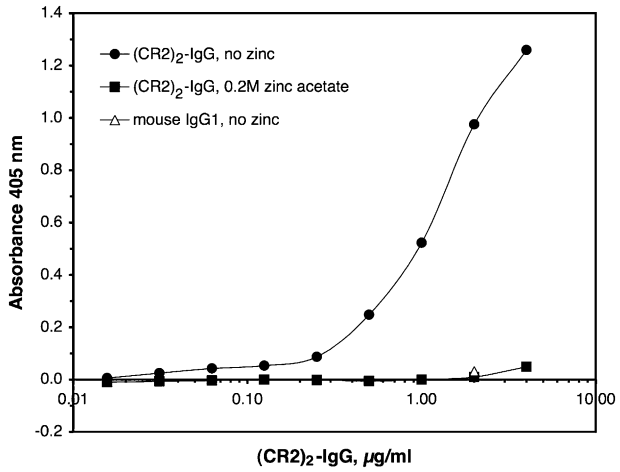

FIGURE 4. ELISA-based binding assay of $(CR2)_2$-IgG to plate-bound C3dg C17A(1010) carried out in the presence and absence of 0.2 M zinc acetate and under pH and ionic strength conditions (see *Materials and Methods*) that mimicked the crystallization conditions for the CR2(SCR1–2):C3d complex (26). The use of the C17A version of C3dg, which in SPR experiments displayed an identical binding affinity for CR2(SCR1–2) as did WT C3dg, was done as a precaution against zinc ions being coordinated by the free cysteine side chain at the thioester position. Also, it was the C17A derivative of C3d that Szakonyi et al. (26) had used to obtain the cocrystal with CR2(SCR1–2) in the presence of the 0.2 M zinc acetate additive. The background level binding of a control mouse IgG1 at 2 μg/ml is also indicated.

favor the detection of complex formed in the presence of 0.2 M zinc acetate, as micromolar zinc has been reported to be slightly stimulatory to the activity of HRP (39). However, the results of the assay carried out using the HRP conjugate exactly mirrored those obtained with the alkaline-phosphatase conjugate (data not shown).

Discussion

Despite the relatively low sequence identity between Sbi-IV and either Efb-C or Ehp (19–23%), all three C3d-binding proteins share similar three-helix bundle domain architecture. Whether it is a result of convergent or divergent evolution, our mutagenesis data strongly suggest that Sbi-IV binds to C3d in a manner very analogous to that visualized in the cocrystal structures of the Efb-C:C3d and the Ehp:C3d complexes (7, 8). In the Efb-C:C3d cocrystal structure, the side chain of Efb-C R131 is tucked into a solvent-lined pocket of C3d consisting of residues H33(1026), D36(1029), N98(1091), and L99(1092) (the number in parentheses is preproC3 numbering). The carboxylate of C3d D36(1029) is within ionic bonding distance (3.1–4.1Å) of the two closest nitrogen atoms of the guanido group of R131. The latter residue is conserved as R231 in Sbi-IV, and we have previously shown that its mutation to alanine is on its own sufficient to completely abrogate the Sbi-IV:C3d interaction (11). Our finding that the D36A mutant C3dg has also lost all Sbi-IV–binding activity suggests that the sides chains of Sbi-IV R231 and C3d D36(1029) form a similar salt bridge to that seen in the Efb-C:C3d complex. Our finding that the R49M(1042) mutant displays the second-largest Sbi-IV–binding defect in the 30s–40s cluster is in keeping with this residue making a weak hydrogen bond with the side chain of H130 of Efb, although the equivalent residue in Sbi-IV is R230, and thus a different type of interaction would be required. The C3d 160s cluster of residues appears to be a secondary interaction site as even the most compromised mutants of C3dg only display a 2- to 3-fold reduction in binding to Sbi-IV. For the D163(1156) alanine mutant, this likely reflects a loss of a salt bridge to the guanido group of R235 as the equivalent lysine residue in Efb does form a salt bridge (~4Å bond length) with D163(1156) of C3d (7). It was suggested that K106 and K107 of the α1-helix of Efb-C, and K148 of its α3-helix, may make fairly long-range, and therefore weak, interactions with acidic residues in C3d 160s cluster (7). The equivalent residues in Sbi-IV are R206, H207, and V244, so the possibility exists of a weak ionic interaction with the two residues of the Sbi-IV α1-helix but not with its α3-helix.

As discussed above, it is fairly clear that like Efb-C and Ehp, Sbi-IV binds to a face of the C3d molecule, namely the one containing the acidic residue-lined concave depression, that our earlier mutagenesis work had implicated as mediating, at least in part, the binding of the SCR1–2 domains of CR2 (24). This would explain why Sbi-IV (Fig. 1) and Efb-C (23) are able to inhibit the CR2(SCR1–2):C3d(g) interaction. But, as alluded to earlier, the CR2(SCR1–2):C3d cocrystal structure shows no interaction of CR2 to this region of the molecule and questions were raised about the validity of our earlier mutagenesis study. For example, it was suggested (36) that our use of mutant forms of iC3b, and not C3d(g), as the ligand could have affected the results, as some studies had indicated that iC3b may bind to CR2 at different sites than C3d(g) (40, 41). Even in our previous study (24), the results for a subset of the mutants had been verified in a rosette assay in which the ligand had been converted to C3dg. However, in the current study, using a larger number of variant C3dg molecules as the ligand and a biophysical readout of the extent of binding to CR2(SCR1–2), we have through totally independent means validated our initial observations on the involvement of resides of the acidic residue-lined concave face of C3d in binding CR2. Indeed, despite the methodological differences, it can be seen in Fig. 5 that the current SPR results largely recapitulate in a quantitative sense the earlier functional assay-derived data. The only substantial differences between the new and old data are for the very modest defects seen by SPR for the D36A (1029) and the R49M(1042) mutants. Whereas the rosette assay measured effects on avidity, C3dg is monomeric under the conditions of our experiment (42), and so the SPR results should be more sensitive to picking up minor differences in intrinsic affinity.

In addition to the previously referred to mutagenic evidence (36) for the involvement of several basic residues of the SCR1 domain of

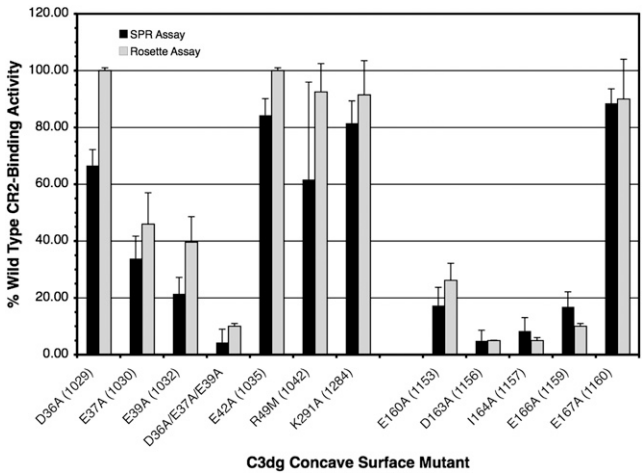

FIGURE 5. Comparison of relative binding to CR2 of mutant C3dg, as assessed by SPR, and of mutant iC3b deposited on red cells and assessed by quantitative rosette assay. The mutations all target residues within the acidic pocket on the concave surface of C3d. The SPR data (■) are from the current study, and the quantitative rosette assay data (gray bars) are from the Clemenza et al. 2000 study (24).

CR2 in the interaction with C3d, a very recent study from the same laboratory (43) has used NMR chemical shift analysis of unlabeled C3d titrated into ^{15}N-labeled CR2(SCR1–2) to confirm and extend these results to include several additional SCR1 residues. On the basis of these data, Holers and coworkers now readily concede that the cocrystal structure (26) represents an incomplete picture of the physiological CR2:C3d complex. Nevertheless, they appear to still contend that the CR2(SCR2):C3d interface seen in the cocrystal is correct. The cocrystal structure indicated that the side chain of R83 in SCR2 was the central player in the extensive hydrogen-bond network bridging SCR2 to C3d, and it is true that both the mutagenic (36) and chemical shift perturbation (43) data support the involvement of R83 in binding SCR2 to C3d. In the 2005 study by Hannan et al. (36), it was hypothesized that a cluster of four C3d residues that formed an acidic channel located immediately adjacent to the area visualized as the contact area for SCR2 in the cocrystal structure could provide the direct interaction site for SCR1 that for unknown reasons was absent in the cocrystal structure. We have now tested this hypothesis by doing an alanine mutagenic scan of these residues but have found no evidence for their involvement in CR2 binding.

Obviously, the residues comprising the acidic depression on the concave face of the C3d molecule, which we have now reconfirmed through independent means as being important for the binding of CR2, merit strong consideration as the binding interface for SCR1. Indeed, this appears to be what the authors of a recent study were invoking as an explanation for the competition they observed between Efb-C and CR2 for an overlapping binding site on C3d (23). Specifically, Ricklin et al. (23) depict a model, which is in turn based on a top-ranking model of the C3d:CR2(SCR1–2) complex derived from analysis of small angle X-ray scattering data (44) (Protein Data Bank code 1W2S), that retains the SCR2:C3d interface seen in the cocrystal but has the overall conformation of CR2(SCR1–2) adopting an open V conformation, thereby allowing SCR1 to lie in the proximity of the Efb-C binding site on C3d. However, the SCR1:C3d interface in the 1W2S model is on the periphery of the acidic residue lined depression and would not be making close contact with most of the residues identified as being important for CR2 binding in our mutagenic analyses (Ref. 24 and the current study). Our attempts at docking SCR1 farther down into the acidic pocket in a way that tried to provide charge complementarity between residues identified through mutagenesis on both sides of the interface, while maintaining the SCR2:C3d interface as visualized in the cocrystal structure, indicated that it was not possible to do so without breakage of a peptide bond in the linker region joining SCR1 and SCR2 and creating a gap that would require at least another eight residues of linker sequence to be bridged (our unpublished observation). However, there are several new facts that raise doubts about the correctness (in terms of the physiologic complex) of the SCR2:C3d interface visualized in the cocrystal structure. First and foremost, substitution of C3d N170(1163) by alanine, thereby removing the sole side chain-side chain interaction between C3d and SCR2 (to Y80) seen in the cocrystal structure, had absolutely no effect on the ability of the mutant C3dg to bind to CR2. Not only is this result discordant with the structural data, but at first blush, it is also discordant with mutagenesis data involving C3d N170 in the Szakonyi et al. (26) paper that purported to provide support for the visualized interface. However, unlike the situation for the simple alanine substitution that we made at N170, there are potential problems with both of the C3d mutants involving N170 that were made in the original work and which showed loss of CR2-binding function. In one mutant (mut4), a similar alanine substitution at N170 was made, but it was done in combination with I115R and L116R mutations. The bulk of the side chain of I115 is buried, and thus, the introduction of a longer and positively charged side chain at this position is very likely to be problematic with respect to the stability of such a triple-mutant C3d molecule. Mut2 was a single residue substitution of the fully exposed side chain of N170, but here too, the substituting residue used was arginine. As can be seen in Figs. 2*C* and 3*B*, *right panels*, the side chain of N170 is in close proximity to E167(1160), the residue marking the outer boundary of the 160s cluster of residues that we have shown are vital for CR2 binding to C3dg. The positively charged terminus of the arginine side chain, together with its additional length (~4.5Å) relative to the asparagine side chain, may well facilitate an intramolecular ionic interaction with acidic residues in the 160s cluster that may interfere with the ability of these residues to participate in making contacts to CR2. We have previously noted that positive charges in the 160s cluster region of C3d have a negative effect on CR2 binding as the substitution of K162(1155) by alanine lead to an increase in CR2-binding activity (24).

There are two additional results in the recently published NMR chemical shift perturbation data (43) referred to above that in our view raise further questions about the correctness of the CR2 (SCR2):C3d interface visualized in the cocrystal structure. In the NMR study, the authors characterize all of the interactions between C3d and SCR1 detected by chemical shift perturbation as being of a tight binding nature, whereas those to SCR2 and the linker region were of weaker affinity. This then begs the question of how to rationalize the retention under the constraints of crystal packing of the weak binding interface and not the strong binding interface. An additional point derived from the NMR study was that in addition to SCR2 residues R83 and G84, for which this group had previously provided mutagenesis evidence supporting their involvement in binding to C3d (36), 11 additional residues on the same face of SCR2 as R83 and G84 were reported as being perturbed upon the addition of C3d. Conspicuously missing from the list, however, is Y80, the residue visualized in the CR2(SCR1–2):C3d cocrystal structure as interacting with C3d N170 and contributing the sole side chain-side chain interaction of the interface.

From the very beginning, the CR2(SCR1–2):C3d cocrystal structure (26) has been at odds with a large body of pre-existing biochemical data. Moreover, subsequent publications that were either from the same group as published the cocrystal structure, or involved them as major collaborators, only served to further highlight the discrepancies. Besides the points already alluded to as being discrepant with the biochemical data (i.e., the lack of C3d contact with SCR1, the absence of any classical salt bridges, and the paucity of side chain-side chain interactions at the interface to confer specificity), there were also issues with respect to the stoichiometry of the complex and the very acute angle between the SCR1 and SCR2 domains. Specifically, the stoichiometry of the cocrystal complex is two CR2(SCR1–2) to one C3d, and the CR2 moiety shows a head to head dimer interface mediated by SCR1. By contrast, both an independent crystal structure of free CR2 (SCR1–2) (28), as well as analytical ultracentrifugation data on the same CR2(SCR1–2) protein used in the cocrystallization with C3d (32), unambiguously indicated that the protein was monomeric in solution. Furthermore, analytical ultracentrifugation data for the CR2(SCR1–2):C3d complex were consistent with a 1:1 stoichiometry (32). The closed V-shaped arrangement of SCR1 and SCR2 domains seen in the cocrystal structure in which there are extensive interdomain contacts is inconsistent with 1) the hydrodynamic data for free CR2(SR1–2) in solution (32), 2) a model of the CR2(SCR1–2):C3d complex based on X-ray scattering data (44), and 3) the steric clash that would occur between the SCR1 interface and a physiologic length glycan chain

that would normally be attached to Asn^{107} of SCR2 (28), all of which point to a more extended open-V conformation between SCR1 and SCR2 and with no interdomain contacts. If one adds to this list of biochemical inconsistencies our present findings regarding the confirmation of the acidic residue-lined depression on the concave surface of C3d as a major CR2 binding site that was not visible in the cocrystal structure, the ability of contacts at this site to explain the competition observed between CR2 and Sbi-IV (Fig. 1) or Efb-C (23) for binding to C3d, and the failure to confirm the involvement of C3d N170(1163) in binding CR2, it leaves only the individual domain structures of C3d, SCR1, and SCR2 as elements of the cocrystal structure that are consistent with data in the literature.

Prota et al. (28) have previously noted that the presence of 0.2 M zinc acetate in the crystallization medium has resulted in there being two nonphysiologic zinc atoms at the C3d:CR2 interface of the cocrystal structure. They wondered whether amino acids involved in contacting these zinc ions might otherwise have been available to make additional physiologically relevant contacts not seen in the cocrystal structure. We observed that inclusion of 0.2 M zinc acetate in the binding buffer essentially eliminated the CR2(SCR1–2):C3dg interaction, whereas an isoionic buffer at the same pH permitted robust binding (Fig. 4). This then raises the distinct possibility that the C3d and CR2(SCR1–2) molecules visualized in the cocrystal structure (26) in essence crystallized as noninteracting entities and that the contacts seen between them derive from favorable crystal packing energetics. Specifically, the tight crystal packing interactions are seen mainly to occur through CR2-CR2 contacts. These involve "head-to-head" interactions between two SCR1 domains in the asymmetric unit (buried surface area [b.s.a.] 962 $Å^2$) and antiparallel interactions between the SCR1 domain and its counterpart domain in a symmetry-related CR2 molecule (b.s.a. 728 $Å^2$). These entropically favorable interactions between the CR2 molecules, adding up to a total b.s.a. of ~1700 $Å^2$ and additionally aided by the SCR1-SCR2 interdomain interactions (b.s.a. 809 $Å^2$ for the C3d-contacting CR2 molecule and 835 $Å^2$ for the second CR2 molecule in the asymmetric unit) that are possible because of the absence of the normal carbohydrate chain (28), may have driven the formation of the molecular lattice observed in the structure. Recently, a large-scale computational docking experiment has been performed to estimate the extent of misrepresentation of protein-protein interfaces because of crystal packing effects. Using protein dimer interfaces as a subset of the general case, it was reported that for weakly associated complexes having a $K_D \geq 100$ μM, as would certainly be the case for the C3d:CR2(SCR1–2) complex in the presence of 0.2 M zinc acetate at pH 6.26, the chances of misrepresentation in the crystalline state of the physiologically relevant protein-protein interface was on the order of 85–90% (45). We are currently endeavoring to obtain independent crystals of the CR2(SCR1–2):C3d complex in the hope of obtaining a structural model of the complex that will be more consistent with the large body of biochemical data that is currently available.

In summary, we have explored via site-directed mutagenesis a putative binding interface on C3d for the Sbi-IV domain of the staphylococcal immune evasion molecule Sbi. Our results strongly suggest that Sbi-IV binds C3d in a manner that is highly similar to what was seen in the cocrystal structures of C3d with Efb-C (7) and Ehp (8), the functional *Staphylococcus aureus* homologs of Sbi. This C3d interface, comprising an acidic pocket on the concave surface of C3d, has been confirmed to also be vital for the interaction of C3d with CR2. Although the binding sites for Sbi-IV and CR2 are overlapping, thus allowing the bacterial evasion molecule to block CR2 binding and potentially inhibiting the host's adaptive immune response to the pathogen, there is divergence in the particular residues and subregions of the interface, which appear to be most vital for the respective binding interactions with Sbi-IV and CR2. Finally, we believe that the results of our current study, including the discovery of the inhibitory effect of the zinc acetate crystallization additive on C3d:CR2 complex formation, together with other data in the literature that we have summarized, now render untenable the published CR2(SCR1–2):C3d cocrystal structure as even a starting point for a model of the physiologically relevant interaction.

Acknowledgments

We thank one of the anonymous reviewers of our manuscript for having prodded us to experimentally explore the issue of the zinc acetate additive.

Disclosures

The authors have no financial conflicts of interest.

References

1. Lambris, J. D., D. Ricklin, and B. V. Geisbrecht. 2008. Complement evasion by human pathogens. *Nat. Rev. Microbiol.* 6: 132–142.
2. Langley, R., B. Wines, N. Willoughby, I. Basu, T. Proft, and J. D. Fraser. 2005. The staphylococcal superantigen-like protein 7 binds IgA and complement C5 and inhibits IgA-Fc α RI binding and serum killing of bacteria. *J. Immunol.* 174: 2926–2933.
3. Haas, P. J., C. J. de Haas, M. J. Poppelier, K. P. van Kessel, J. A. van Strijp, K. Dijkstra, R. M. Scheek, H. Fan, J. A. Kruijtzer, R. M. Liskamp, and J. Kemmink. 2005. The structure of the C5a receptor-blocking domain of chemotaxis inhibitory protein of *Staphylococcus aureus* is related to a group of immune evasive molecules. *J. Mol. Biol.* 353: 859–872.
4. Postma, B., M. J. Poppelier, J. C. van Galen, E. R. Prossnitz, J. A. van Strijp, C. J. de Haas, and K. P. van Kessel. 2004. Chemotaxis inhibitory protein of *Staphylococcus aureus* binds specifically to the C5a and formylated peptide receptor. *J. Immunol.* 172: 6994–7001.
5. Rooijakkers, S. H., M. Ruyken, A. Roos, M. R. Daha, J. S. Presanis, R. B. Sim, W. J. van Wamel, K. P. van Kessel, and J. A. van Strijp. 2005. Immune evasion by a staphylococcal complement inhibitor that acts on C3 convertases. *Nat. Immunol.* 6: 920–927.
6. Rooijakkers, S. H., J. Wu, M. Ruyken, R. van Domselaar, K. L. Planken, A. Tzekou, D. Ricklin, J. D. Lambris, B. J. Janssen, J. A. van Strijp, and P. Gros. 2009. Structural and functional implications of the alternative complement pathway C3 convertase stabilized by a staphylococcal inhibitor. *Nat. Immunol.* 10: 721–727.
7. Hammel, M., G. Sfyroera, D. Ricklin, P. Magotti, J. D. Lambris, and B. V. Geisbrecht. 2007. A structural basis for complement inhibition by *Staphylococcus aureus*. *Nat. Immunol.* 8: 430–437.
8. Hammel, M., G. Sfyroera, S. Pyrpassopoulos, D. Ricklin, K. X. Ramyar, M. Pop, Z. Jin, J. D. Lambris, and B. V. Geisbrecht. 2007. Characterization of Ehp, a secreted complement inhibitory protein from *Staphylococcus aureus*. *J. Biol. Chem.* 282: 30051–30061.
9. Burman, J. D., E. Leung, K. L. Atkins, M. N. O'Seaghdha, L. Lango, P. Bernadó, S. Bagby, D. I. Svergun, T. J. Foster, D. E. Isenman, and J. M. van den Elsen. 2008. Interaction of human complement with Sbi, a staphylococcal immunoglobulin-binding protein: indications of a novel mechanism of complement evasion by *Staphylococcus aureus*. *J. Biol. Chem.* 283: 17579–17593.
10. Zhang, L., K. Jacobsson, J. Vasi, M. Lindberg, and L. Frykberg. 1998. A second IgG-binding protein in *Staphylococcus aureus*. *Microbiology* 144: 985–991.
11. Upadhyay, A., J. D. Burman, E. A. Clark, E. Leung, D. E. Isenman, J. M. van den Elsen, and S. Bagby. 2008. Structure-function analysis of the C3 binding region of *Staphylococcus aureus* immune subversion protein Sbi. *J. Biol. Chem.* 283: 22113–22120.
12. Nagar, B., R. G. Jones, R. J. Diefenbach, D. E. Isenman, and J. M. Rini. 1998. X-ray crystal structure of C3d: a C3 fragment and ligand for complement receptor 2. *Science* 280: 1277–1281.
13. Janssen, B. J., A. Christodoulidou, A. McCarthy, J. D. Lambris, and P. Gros. 2006. Structure of C3b reveals conformational changes that underlie complement activity. *Nature* 444: 213–216.
14. Kalli, K. R., J. M. Ahearn, and D. T. Fearon. 1991. Interaction of iC3b with recombinant isotypic and chimeric forms of CR2. *J. Immunol.* 147: 590–594.
15. Matsumoto, A. K., J. Kopicky-Burd, R. H. Carter, D. A. Tuveson, T. F. Tedder, and D. T. Fearon. 1991. Intersection of the complement and immune systems: a signal transduction complex of the B lymphocyte-containing complement receptor type 2 and CD19. *J. Exp. Med.* 173: 55–64.
16. Fearon, D. T., and R. H. Carter. 1995. The CD19/CR2/TAPA-1 complex of B lymphocytes: linking natural to acquired immunity. *Annu. Rev. Immunol.* 13: 127–149.
17. Cherukuri, A., R. H. Carter, S. Brooks, W. Bornmann, R. Finn, C. S. Dowd, and S. K. Pierce. 2004. B cell signaling is regulated by induced palmitoylation of CD81. *J. Biol. Chem.* 279: 31973–31982.

18. Cherukuri, A., T. Shoham, H. W. Sohn, S. Levy, S. Brooks, R. Carter, and S. K. Pierce. 2004. The tetraspanin CD81 is necessary for partitioning of coligated CD19/CD21-B cell antigen receptor complexes into signaling-active lipid rafts. *J. Immunol.* 172: 370–380.
19. Cherukuri, A., P. C. Cheng, H. W. Sohn, and S. K. Pierce. 2001. The CD19/CD21 complex functions to prolong B cell antigen receptor signaling from lipid rafts. *Immunity* 14: 169–179.
20. Roozendaal, R., and M. C. Carroll. 2007. Complement receptors CD21 and CD35 in humoral immunity. *Immunol. Rev.* 219: 157–166.
21. Dempsey, P. W., M. E. Allison, S. Akkaraju, C. C. Goodnow, and D. T. Fearon. 1996. C3d of complement as a molecular adjuvant: bridging innate and acquired immunity. *Science* 271: 348–350.
22. Carroll, M. C. 2000. The role of complement in B cell activation and tolerance. *Adv. Immunol.* 74: 61–88.
23. Ricklin, D., S. K. Ricklin-Lichtsteiner, M. M. Markiewski, B. V. Geisbrecht, and J. D. Lambris. 2008. Cutting edge: members of the *Staphylococcus aureus* extracellular fibrinogen-binding protein family inhibit the interaction of C3d with complement receptor 2. *J. Immunol.* 181: 7463–7467.
24. Clemenza, L., and D. E. Isenman. 2000. Structure-guided identification of C3d residues essential for its binding to complement receptor 2 (CD21). *J. Immunol.* 165: 3839–3848.
25. Hannan, J., K. Young, G. Szakonyi, M. J. Overduin, S. J. Perkins, X. Chen, and V. M. Holers. 2002. Structure of complement receptor (CR) 2 and CR2-C3d complexes. *Biochem. Soc. Trans.* 30(Pt. 6): 983–989.
26. Szakonyi, G., J. M. Guthridge, D. Li, K. Young, V. M. Holers, and X. S. Chen. 2001. Structure of complement receptor 2 in complex with its C3d ligand. *Science* 292: 1725–1728.
27. Hebell, T., J. M. Ahearn, and D. T. Fearon. 1991. Suppression of the immune response by a soluble complement receptor of B lymphocytes. *Science* 254: 102–105.
28. Prota, A. E., D. R. Sage, T. Stehle, and J. D. Fingeroth. 2002. The crystal structure of human CD21: Implications for Epstein-Barr virus and C3d binding. *Proc. Natl. Acad. Sci. USA* 99: 10641–10646.
29. Ho, S. N., H. D. Hunt, R. M. Horton, J. K. Pullen, and L. R. Pease. 1989. Site-directed mutagenesis by overlap extension using the polymerase chain reaction. *Gene* 77: 51–59.
30. Krissinel, E., and K. Henrick. 2007. Inference of macromolecular assemblies from crystalline state. *J. Mol. Biol.* 372: 774–797.
31. Moore, M. D., R. G. DiScipio, N. R. Cooper, and G. R. Nemerow. 1989. Hydrodynamic, electron microscopic, and ligand-binding analysis of the Epstein-Barr virus/C3dg receptor (CR2). *J. Biol. Chem.* 264: 20576–20582.
32. Guthridge, J. M., J. K. Rakstang, K. A. Young, J. Hinshelwood, M. Aslam, A. Robertson, M. G. Gipson, M. R. Sarrias, W. T. Moore, M. Meagher, et al. 2001. Structural studies in solution of the recombinant N-terminal pair of short consensus/complement repeat domains of complement receptor type 2 (CR2/CD21) and interactions with its ligand C3dg. *Biochemistry* 40: 5931–5941.
33. Diefenbach, R. J., and D. E. Isenman. 1995. Mutation of residues in the C3dg region of human complement component C3 corresponding to a proposed binding site for complement receptor type 2 (CR2, CD21) does not abolish binding of iC3b or C3dg to CR2. *J. Immunol.* 154: 2303–2320.
34. Lowell, C. A., L. B. Klickstein, R. H. Carter, J. A. Mitchell, D. T. Fearon, and J. M. Ahearn. 1989. Mapping of the Epstein-Barr virus and C3dg binding sites to a common domain on complement receptor type 2. *J. Exp. Med.* 170: 1931–1946.
35. Molina, H., S. J. Perkins, J. Guthridge, J. Gorka, T. Kinoshita, and V. M. Holers. 1995. Characterization of a complement receptor 2 (CR2, CD21) ligand binding site for C3. An initial model of ligand interaction with two linked short consensus repeat modules. *J. Immunol.* 154: 5426–5435.
36. Hannan, J. P., K. A. Young, J. M. Guthridge, R. Asokan, G. Szakonyi, X. S. Chen, and V. M. Holers. 2005. Mutational analysis of the complement receptor type 2 (CR2/CD21)-C3d interaction reveals a putative charged SCR1 binding site for C3d. *J. Mol. Biol.* 346: 845–858.
37. Reichle, R. A., K. G. McCurdy, and L. G. Helper. 1975. Zinc hydroxide: Solubility product and hydroxy-complex stability constants from 12.5–75°C. *Can. J. Chem.* 53: 3841–3845.
38. Townshend, A., and A. Vaughan. 1969. Applications of enzyme-catalysed reactions in trace analysis-IV Determination of beryllium and zinc by their inhibition of calf-intestinal alkaline phosphatase. *Talanta* 16: 929–937.
39. Coteur, G., and P. Dubois. 2004. Interaction of metals with peroxidase-mediated luminol-enhanced, chemiluminescence (PLmCL). *Luminescence* 19: 283–286.
40. Esparza, I., J. D. Becherer, J. Alsenz, A. De la Hera, Z. Lao, C. D. Tsoukas, and J. D. Lambris. 1991. Evidence for multiple sites of interaction in C3 for complement receptor type 2 (C3d/EBV receptor, CD21). *Eur. J. Immunol.* 21: 2829–2838.
41. Sarrias, M. R., S. Franchini, G. Canziani, E. Argyropoulos, W. T. Moore, A. Sahu, and J. D. Lambris. 2001. Kinetic analysis of the interactions of complement receptor 2 (CR2, CD21) with its ligands C3d, iC3b, and the EBV glycoprotein gp350/220. *J. Immunol.* 167: 1490–1499.
42. Li, K., A. I. Okemefuna, J. Gor, J. P. Hannan, R. Asokan, V. M. Holers, and S. J. Perkins. 2008. Solution structure of the complex formed between human complement C3d and full-length complement receptor type 2. *J. Mol. Biol.* 384: 137–150.
43. Kovacs, J. M., J. P. Hannan, E. Z. Eisenmesser, and V. M. Holers. 2009. Mapping of the C3d ligand binding site on complement receptor 2 (CR2/CD21) using nuclear magnetic resonance and chemical shift analysis. *J. Biol. Chem.* 284: 9513–9520.
44. Gilbert, H. E., J. T. Eaton, J. P. Hannan, V. M. Holers, and S. J. Perkins. 2005. Solution structure of the complex between CR2 SCR 1-2 and C3d of human complement: an X-ray scattering and sedimentation modelling study. *J. Mol. Biol.* 346: 859–873.
45. Krissinel, E. 2010. Crystal contacts as nature's docking solutions. *J. Comput. Chem.* 31: 133–143.